Electric Power Systems Research 251 (2026) 112220

Contents lists available at ScienceDirect

Electric Power Systems Research

journal homepage: www.elsevier.com/locate/epsr

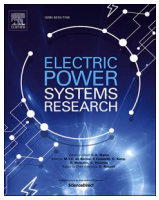

Ferroresonance identification by pattern recognition of its characteristic wavelets

Aminat B. Rasheed [a], Jose de Jesus Chavez [b,*], Sarasij Das [c], Oliver Probst [b], Juan Carlos Cisneros Ortega [b], Marjan Popov [d]

[a] Volker Energy Solutions, Boompjes 40, Rotterdam 3011 XB, the Netherlands
[b] Tecnologico de Monterrey, Escuela de Ingeniería y Ciencias, Ave. Eugenio Garza Sada 2501, Sur, Col: Tecnológico, Monterrey, N.L. 64700, Mexico
[c] Department of Electrical Engineering, Indian Institute of Science, Bangalore, Karnataka 560012, Utkarsh Singh, India
[d] Faculty of Electrical Engineering, mathematics and Computer Science, Delft University of Technology, Delft CD2628, the Netherlands

ARTICLE INFO

Keywords:
Ferroresonance
Fault identification
Electromagnetic transients
Pattern recognition

ABSTRACT

Ferroresonance, a non-linear and unpredictable disturbance, is rare compared to traditional power system faults occurring in power systems. This rarity, coupled with its complexity, makes it a challenging phenomenon to be detected and identified. This work presents a detection and classification scheme for ferroresonance and its modes. It is carried out by continuously processing the three-phase voltage and current signals using the discrete wavelet transform (DWT). The developed models are simulated in electromagnetic transient software and processed using the DWT to extract fault signatures and predictors. A decision tree classifier is trained to detect and classify a disturbance as ferroresonance using an adaptive time based on the disturbance class. The computational burden of the detection and classification process is significantly reduced by using the superimposed component of the voltage and current to detect transient inceptions before classification. Furthermore, the classification of different modes and classification from other non-linear faults, such as arcing faults, is discussed. The adaptive timing and detection scheme demonstrates that the proposed methodology is efficient and can classify the disturbance into different modes.

1. Introduction

THE electrical power system is the most complex man-made systems on earth. The continuing rise in energy demand, today's emphasis on greener, more sustainable electricity generation, and the regulations to provide high-quality and affordable energy always add further complexity to power system studies. The impact of disturbances on power grids depends on the event nature, location, severity level, system design, interconnection network downstream, and protection system. Although primary and backup protection schemes are designed to reduce the impact of disturbances, certain faults are inherently difficult to detect or identify. The constantly growing power system must be able to handle all kinds of disturbances, including those produced by inverter-based resources (IBR) from wind farms, solar power plants, and battery energy storage systems (BESS). Wind and solar plants to ensure continuity of service to the users.

Ferroresonance is one of the phenomena that is difficult to detect or identify by actual protection devices. In fact, it is a complex and unpredictable phenomenon in power systems caused by nonlinear interactions between transformers, reactors, and surrounding capacitances resulting from cables and lines [1]. It can lead to severe overvoltage, equipment damage, and insulation breakdown, posing significant risks to system reliability and safety. Detecting and mitigating ferroresonance is challenging due to its dependence on system conditions, such as switching operations or abnormal configurations, which makes it difficult to predict or control. Therefore, a resilient monitoring system is needed to complement the action of protection relays and securely protect the network from this kind of disturbance. Different studies have been carried out to understand the ferroresonance phenomenon in power systems since the term was coined in 1920 by P. Boucherot [2]. The different circuit configurations vulnerable to ferroresonance occurrence are discussed in [3], including experimental and real-life cases of occurrence of this phenomenon. Similarly, research was conducted on detecting ferroresonance in power systems, discriminating

* Corresponding author.
E-mail addresses: J.J.ChavezMuro@tec.mx (J.J. Chavez), sarasij@iisc.ac.in (S. Das), oprobst@tec.mx (O. Probst), juancarlos.cisneros@tec.mx (J.C.C. Ortega), M.Popov@tudelft.nl (M. Popov).

https://doi.org/10.1016/j.epsr.2025.112220
Received 3 January 2025; Received in revised form 13 February 2025; Accepted 4 September 2025
Available online 10 September 2025

the event against other switching transients like capacitor switching, transformer switching and load switching. In [4], the Wavelet Transform (WT) was used for signal decomposition and the Learning Vector Quantizer (LVQ) neural network for classification over other disturbances. In [5], the Stockwell transform (S-transform) was used for feature extraction and support vector machine (SVM) to distinguish ferroresonce events from other transients. In [6], the authors used WT for signal decomposition and feature extraction and then proceeded to employ a decision tree to determine a ferroresonance among other events. The approaches discussed in [4] and [6] were found to be not robust enough to distinguish ferroresonance modes. Moreover, wavelet decomposition presents a high value at the inception of all transients and is not unique to only ferroresonance occurrence. Later on, by applying an artificial neural network with multi-layer perceptron (MLP) for classification combined with WT, the ferroresonace is identified and differentiated in [7], however, there is no classification in terms of ferroresonance modes. Classification of fundamental and high-frequency ferrroresonances was done in [8] where an improved Elman-Adaboost method is used for classification and identification. In [9], by using the Deep learning approach, the authors reported that the most difficult ferroresonance mode had been identified, the chaotic. Nevertheless, the signals reported in [9] correspond to a transitional chaotic phenomenon but not a chaotic mode.

The methods discussed above focused on distinguishing ferroresonance phenomena from other transient events. The most recent methods use artificial intelligence [6–9], and a few of them [8,9] can classify the ferroresonance in a few modes. In contrast, this work introduces a method that can distinguish and classify the ferroresonance in all its possible modes just after a few cycles of its occurrence. This allows for a nuanced approach to managing this phenomenon, ensuring that the power systems remain stable, efficient, and safe under various operating conditions. It aids in decision-making to prevent and mitigate the future occurrence of this disturbance. Once the fundamental mode is detected, the tailored mitigation strategy must be focused on damping and load adjustments. If quasi-periodic and subharmonic modes are detected, non-linearities and resonances from near nodes must be avoided. Robust protective relays and system isolation strategies may be implemented when chaotic mode is detected.

The developed approach is designed to assist transmission and distribution operators in identifying and classifying ferroresonance, filling an existing gap in identification tools. It enables early detection of specific ferroresonance modes, promoting proactive monitoring to mitigate potential damage.

2. Ferroresonance modes and modeling

In [10], the ferroresonance phenomenon is defined as an unusual anomaly characterized by overvoltage and quite irregular electrical signals. It is associated with the excitation of one or more saturable inductors through capacitance in series. However, resonance could be produced by an arrangement in parallel or series, depending on the network topology. When a resonance occurs in a system, the resonant frequency is deterministic due to the capacitor's and inductor's nature. In contrast, ferroresonance does not occur at a fixed frequency. The inductor, with non-linear behaviour, can have different values in the saturation region of the ferromagnetic material. This implies that different capacitance values can potentially cause ferroresonance at a given frequency [11]. The event can be listed depending on the modes and its characteristic waves, as mentioned in [12] and explained in the next subsections.

2.1. Ferroresonance network configuration

Five network configurations that potentially produce a ferroresonance [13] are: 1) A transformer accidentally energized through only one or two phases, 2) a transformer energized by a capacitive load due to a switch opening, 3) a transformer connected to a series compensated transmission line 4) a transformer connected to a system with an isolated neutral in distribution systems, and 5) a coupling capacitive voltage transformer connected to a non-energized line in parallel to a long line energized or a cable with small short circuit power Among all the possible systems, in this work, the network shown in Fig. 1 has been selected to reproduce and analyze the ferroresonance events. The system consists of a source connected to a line, which at the end is connected to a nonlinear inductor in parallel to a capacitor, a linear load, and a set of three one-phase, three-winding transformers. The model is built in EMTP-ATP environment. The parameters of each element can be found in Table 1.

2.2. Fundamental mode

Fig. 2 shows the evolution of a fundamental ferroresonance event. At the beginning, the signals show a fundamental frequency sinusoidal shape; then the event happens at 0.2 s;-after that, an electromagnetic transient starts and lasts from 0.25 s to 0.5 s (from 0.2 s until 0.7 s).

Thereafter, the voltage and current signals exhibit steady, non-sinusoidal shapes. Fig. 2 signals are obtained by using the model depicted in Fig. 1 and the parameters used in Table 1.

2.3. Quasi-periodic mode

The quasi-periodic mode is not strictly periodic; instead, it exhibits oscillations with multiple frequencies that may not be integer multiples of each other. The oscillations result in complex patterns that never repeat exactly, leading to a quasiperiodic response. For example, the frequency spectrum of the voltage and current is shown in Fig. 3. At least two dominant frequencies exist in the spectrum of the voltage and current; the fundamental (50 Hz) and the third harmonic (150 Hz). Due to the nonlinear behaviour, this mode also contains several frequencies, not multiples of the fundamental frequency (interharmonics), such as 65 Hz, 135 Hz and 165 Hz, along with a subharmonic of 35 Hz.

2.4. Sub-harmonic mode

The subharmonic mode of ferroresonance is dominated by submultiples of the fundamental frequency, as seen in Fig. 4. The dominant frequency f_o/n is a subharmonic of period-n where f_0 is the fundamental frequency. Fig. 4(b) and Fig. 4(d) reveal that the ferroresonance, in this case, is a period 3 subharmonic. The spectrum has a fundamental frequency of 16.67 Hz ($50\ Hz/3$).

To obtain the signals presented in Fig. 4, the system depicted in Fig. 1 with the parameters in Table 1 is used except for the non-linear load, whose values are $I = 2.15$ mA and Flux =725.15 Vs, and the shunt resistance $R = 50$ MΩ.

2.5. Chaotic mode

In chaotic ferroresonance, the signal exhibits random behavior without any discernible pattern. This transient nature persists throughout the signal's duration, lacking uniformity or regularity. The voltage and current spectral components, as shown in Fig. 5(b) and Fig. 5(d), further emphasize this chaotic behavior. Although spikes are noticeable at fundamental and subharmonic frequencies, the broadband nature of the spectrum poses a significant challenge in identifying chaos within the signals, as illustrated in Fig. 5(a) and Fig. 5(c). To obtain the signals in Fig. 5, the system depicted in Fig. 1 with the parameters in Table 1 is used except for the shunt resistance $R = 50$ MΩ and the shunt capacitance C1=0.00045μF.

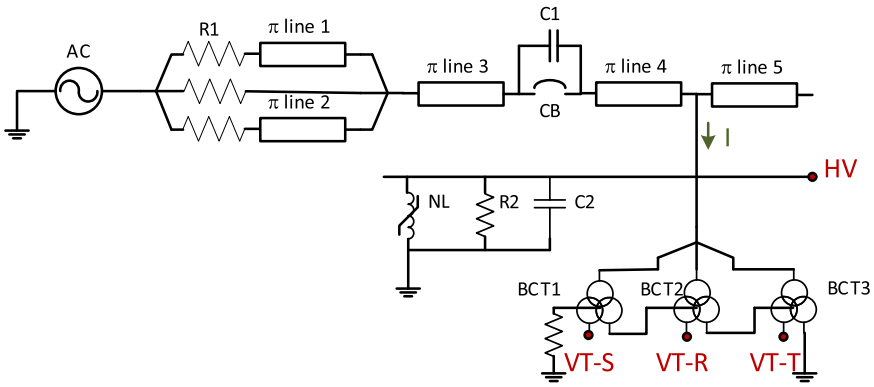

Fig. 1. Schematic model simulated in EMTP-ATP Model to analyze the fundamental, the sub-harmonic and the transitional chaotic (close to chaotic ferroresonance) ferroresonance modes.

Table 1
Ferroresonance network element parameters.

Element	Name *			
Source	AC	$V = 32.4\ kV$	$f = 50$ Hz	
π line 1∅	π line 1	$R = 1.659e4\ \Omega/m$	$L = 3.09e\text{-}6$ mΩ/m	$C = 6.08e\text{-}5$ μF/m
π line 1∅	π line 2	$R = 3.318e4\ \Omega/m$	$L = 8.18e\text{-}6$ mΩ/m	$C = 1.216e\text{-}4$ μF/m
π line 3∅	π line 3			
Capacitor	C1	C_{ABC}=0.0006μF		
Non-linear load 3∅	NL	$I = 3.002$mA	Flux =135.105 Vs	See Table 3
Capacitor	C23	C_{ABC}=0.00027μF		
Resistance	R2	$R = 75$MΩ		
1∅ 3 windings transformer	BCT 1	HV	LV	TV
	BCT 2	$V = 400$ kV	$V = 0.1$ kV	$V = 0.033$ kV
	BCT 3	$P = 0.1$ kVA	$P = 0.1$ kVA	$P = 0.1$ kVA

* Names of the elements correspond to Fig. 1
**All π lines are 1 m length.

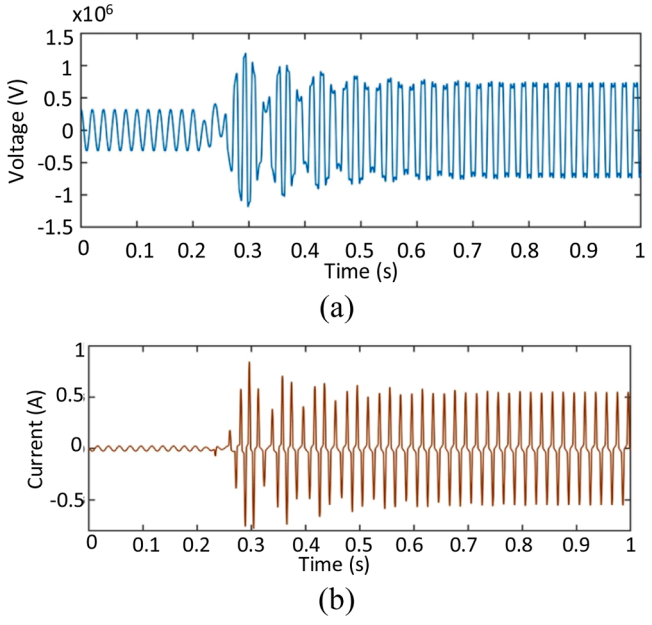

Fig. 2. Fundamental ferroresonance (a) voltage and (b) current waveforms.

3. Methodology

3.1. Discrete wavelet transforms

The discrete wavelet transform (DWT) is widely used in various applications for signal processing and analysis. It is particularly effective for signals with frequency content that varies over time. The DWT transforms time-dependent signals into wavelets, allowing for the identification of important signal features.

The significant advantages of using DWT as the first step in the proposed method are:

- They function as discrete filters. Electrical signals from the field often come with high frequencies and noise that do not pertain to the ferroresonance phenomenon. Thus, these techniques highlight key characteristics of the signals.
- They decompose signals across different scales; low and medium frequencies [14] are utilized for the method, as high frequencies do not correspond to ferroresonance.
- They facilitate the visualization of abrupt changes that may not be apparent in the time domain.
- They are particularly effective for non-stationary signals [15] and can follow the evolution of the ferroresonance.
- They are the preferred method for analyzing signals with rapid peaks and discontinuities, as they can approximate data within a finite domain.
- Individual wavelets are localized in space, making it possible to analyze transient signals resulting from disturbances.

In this document, the signals are transformed using the Daubechies-4 mother wavelet. The detail and approximation coefficients obtained from the wavelet decomposition are utilized as features for the classification algorithm. The choice of the Daubechies-4 mother wavelet over Haar, Fejér–Korovkin, and Symlet wavelets is based on its superior performance during chaotic ferroresonance. This wavelet captures smooth variations, provides excellent noise suppression, enhances frequency resolution, and features a simple structure.

3.2. Step 1: Detection scheme

Superimposed components are used to detect an event. The process runs during the entire simulation time and serves as the starting of the DWT and classification process. Continuous overvoltage and saturation produced during ferroresonance in ferromagnetic equipment require a short time detection to prevent equipment damage. Therefore, a window of one cycle is used to analyze the time series signal of both disturbances. During steady-state conditions, the electrical signal over a time interval of one period (T) should be equivalent to that provided by one cycle

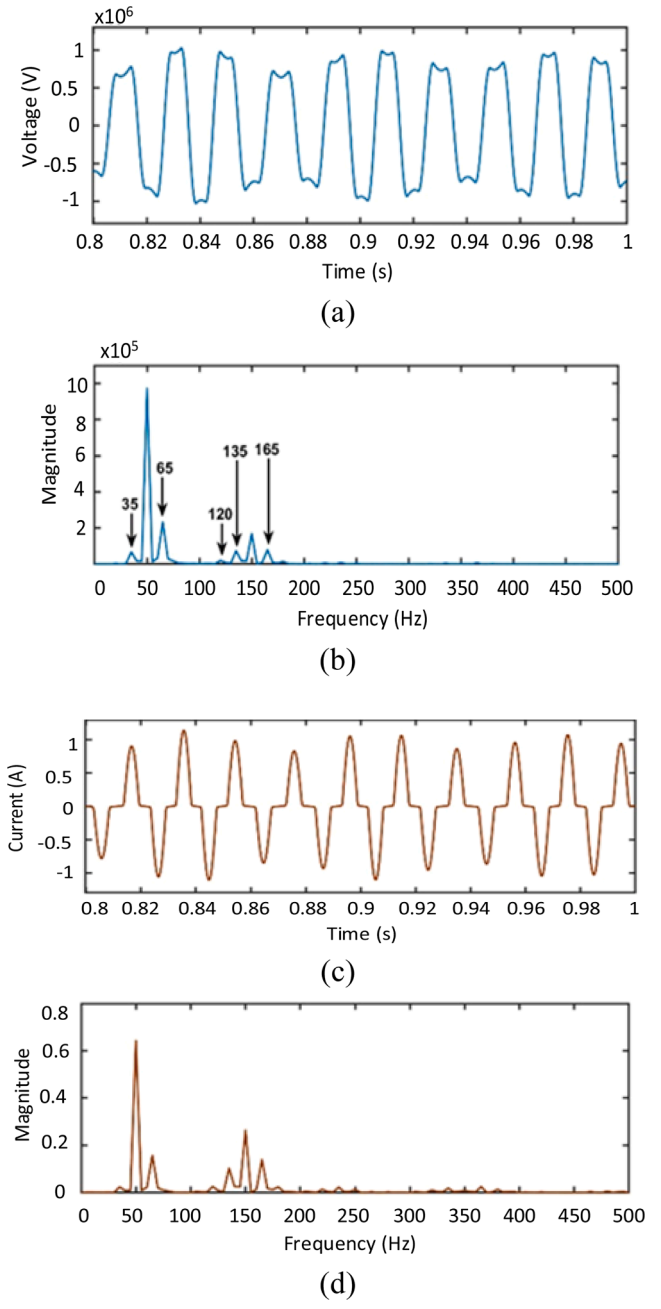

Fig. 3. Quasi-periodic ferroresonance electrical signals and their spectral components (a) voltage, (b) voltage frequency spectra, (c) current, and (d) current frequency spectra.

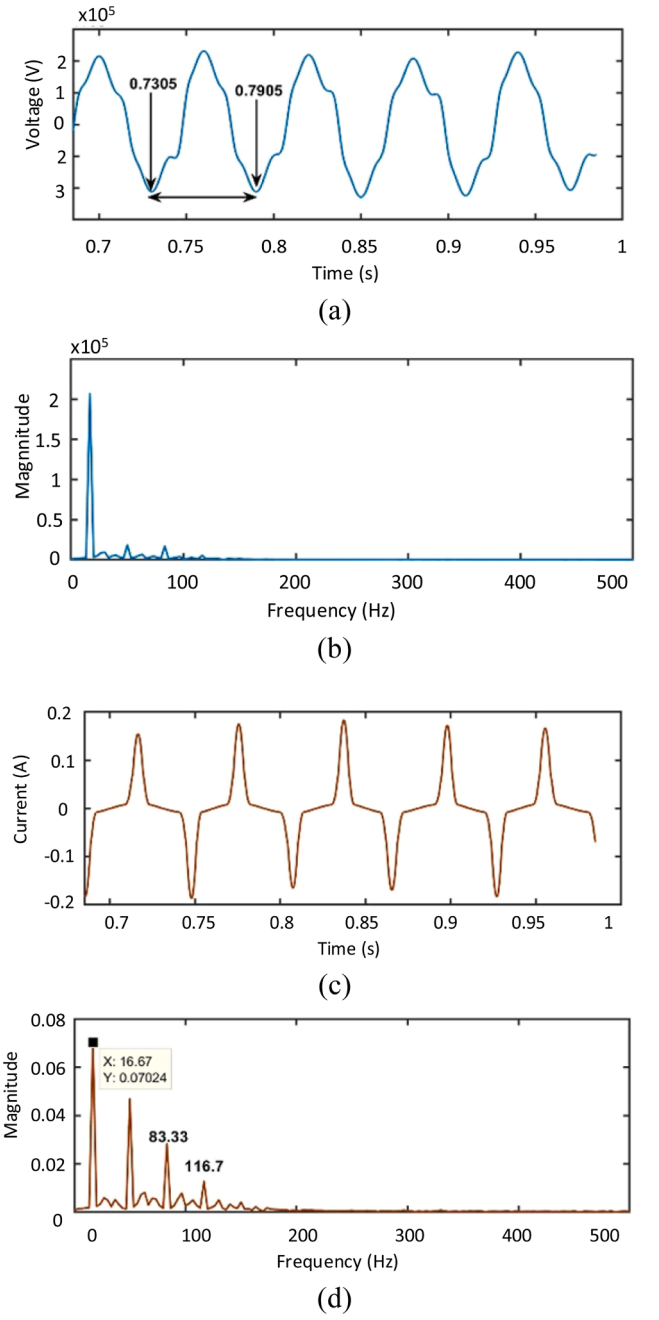

Fig. 4. Sub-harmonic ferroresonance electrical signals and their spectral components (a) voltage, (b) voltage frequency spectra, (c) current, and (d) current frequency spectral.

earlier when there is no external influence or network changes. When a transient condition occurs, at least one of the voltage or current signals presents a value greater or lower than the steady-state value.

The superimposed value of the three-phase currents and voltages are calculated by Eqs. (1) and (2), respectively.

$$\Delta I_{abc}(k) = |I_{abc}(\ k) - I_{abc}(k-T)| \tag{1}$$

$$\Delta V_{abc}(k) = |V_{abc}(\ k) - V_{abc}(k-T)| \tag{2}$$

where T denotes the number of samples per cycle and k is the actual sample. Since the current magnitude of all the disturbances has a wide gap, a combination of superimposed currents and voltages is used to detect the disturbances. A pair of thresholds are then set, one for the current and one for the voltage. The data is normalized to prevent numerical errors in the design using the corresponding voltage and current base for ΔV and ΔI. The equivalent superimposed voltage component is then computed as

$$\Delta V_{abc}(k) = \frac{|V_{abc}(\ k) - V_{abc}(k-T)|}{V_{base}} \tag{3}$$

The superimposed technique adopted in this work to detect disturbances is also used in protective relays [16]. The flow chart in Fig. 6 shows the detection scheme. If the superimposed components present values above the threshold during a hold period (N is the number of samples per period), the disturbance occurrence is confirmed, and the next step in the classification scheme is initiated. The proposed detection scheme is chosen over others for its simplicity and low computational burden. The DWT and other features are extracted in step 2.

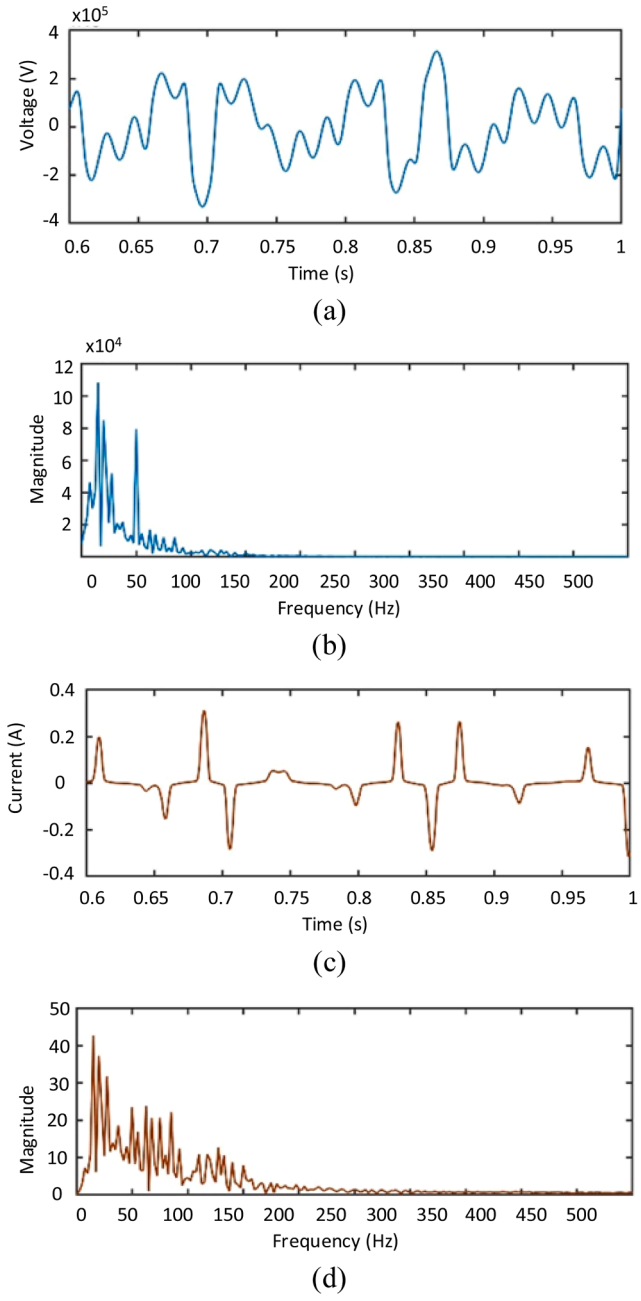

Fig. 5. Chaotic ferroresonance electrical signals and their spectral components (a) voltage, (b) voltage frequency spectra, (c) current, and (d) current frequency spectra.

The phase after the detection is the classification of the disturbances into their corresponding classes. Fig. 7 shows the step-by-step approach adopted in this study.

The features extracted from the processing of DWT outputs in MATLAB are used in the first phase of the classification algorithm to generate the datasets for training and testing.

3.3. Step 2: Machine learning – classification algorithm

Electrical signals during an event are complex to analyze and can sometimes be impossible to classify at first glance, even when the classification is performed offline. Therefore, Machine learning is proposed as a method to classify disturbances. Discrete Wavelet Transform (DWT) is applied to currents and voltages immediately after an event is detected. This process produces detail and approximation coefficients, which

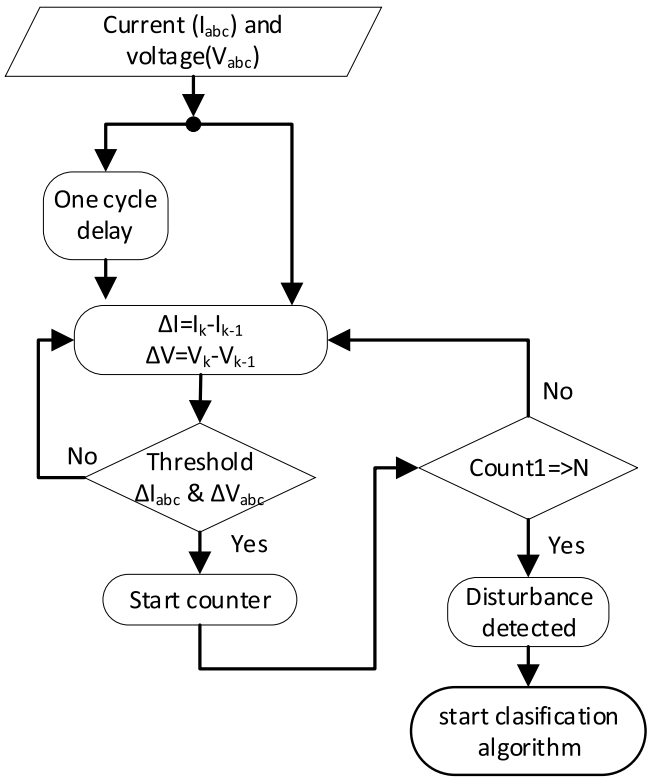

Fig. 6. Disturbance detection flowchart.

are then used to extract features from the various disturbances. The results are stored in a dataset that serves as the training ground for the algorithm.

As discussed in Section II. each type of ferroresonance exhibits distinct harmonic characteristics. With the increasing power of electronic devices in the system, signal distortion also rises. As a result, classifying based solely on harmonic content is no longer feasible. To address this challenge, we utilize the filtering properties and data size reduction capabilities of DWT. Consequently, the resulting signals, only the mother wavelet results, are employed in the machine learning approach.

The algorithm for dataset extraction is developed in Matlab. As inputs, the sampling frequency, DWT's decomposition level, and window size are required. The data labels are generated using the name of each disturbance. The extracted disturbance signal lengths range from 0.35 s to 2 s. To reduce the length of the time series and obtain compact forms of the signals without losing their properties, the signals are partitioned into a shorter length of one cycle (200 samples at f_s=10 kHz) with an overlap of 5 ms (50 samples at f_s=10 kHz). These sets of sequences provide information at different intervals of the original signal that is used as a training dataset to classify the different disturbances as listed.

Fig. 8 shows the step-by-step approach to generate the dataset for a single disturbance class, where *j* represents the index of each simulation. For instance, assuming 20 simulations of the fundamental ferroresonance disturbance in ATPDraw software, then $j = 1, 2, \ldots, 20$. The process is repeated for all the disturbance classes to obtain the total N rows (observations) and M columns (features) dataset. The dataset used here to train the classifier has 32 columns; the first 31 columns represent the features, while the last column represents the class label. Since the datasets are generated sequentially, the matrix rows are arranged randomly. Then, the dataset is divided into two parts: a *training* dataset (75 %) and a *testing* dataset (25 %). The *training* is used to train the algorithm, while the *testing* dataset is used to examine the performance of the trained algorithm.

There are many types of classifiers used for pattern recognition. The

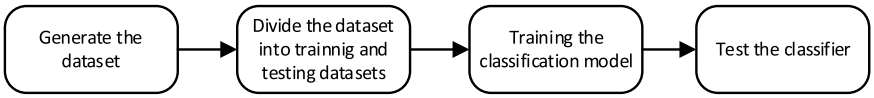

Fig. 7. Flow chart of classification algorithm development.

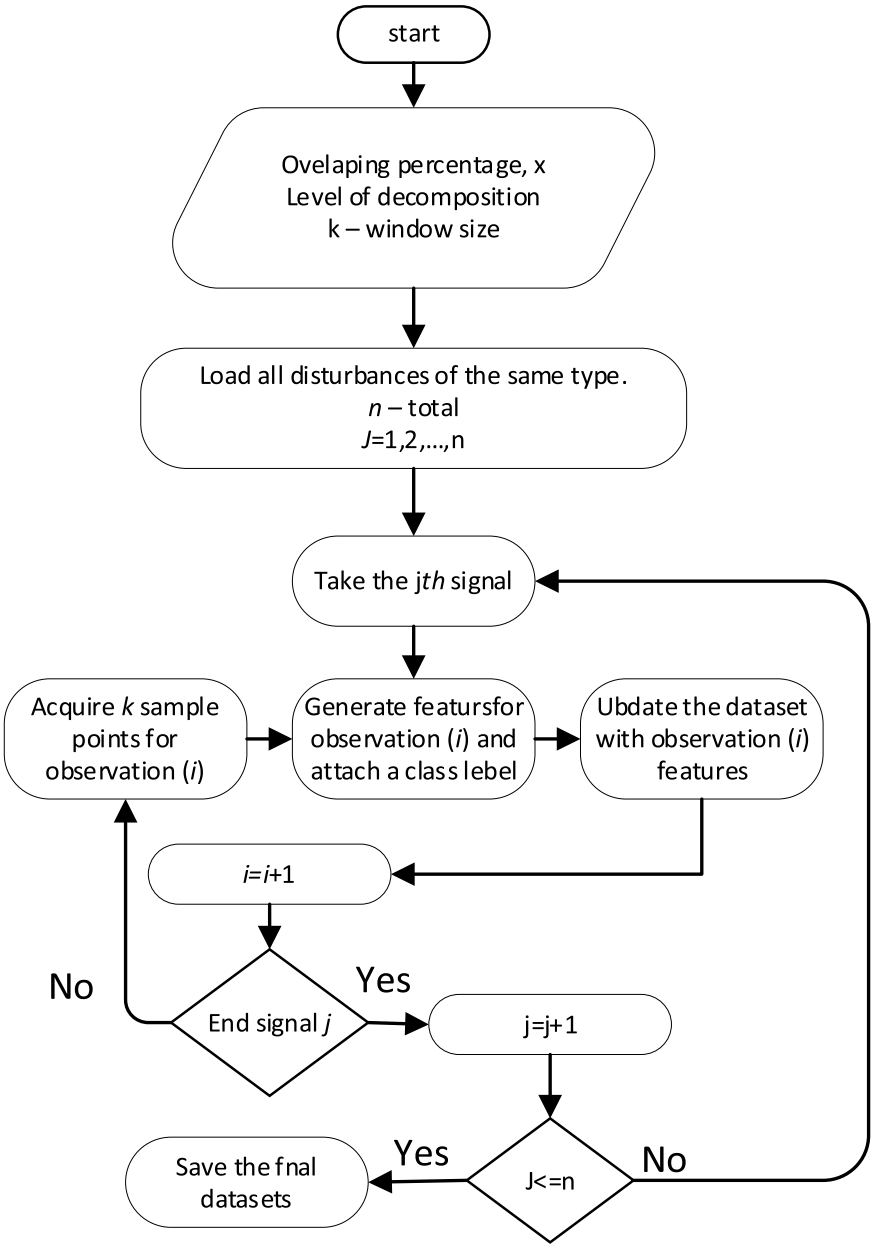

Fig. 8. Step-by-step approach to generate a dataset for all disturbances.

common ones are SVM, decision tree (DT) [17], *k*-nearest neighbor (kNN), naive Bayes classifier, ensemble bagged trees, etc. DT is adopted in this work because of its speed and training time, simplicity, and accuracy [18]. After careful observation and several training processes, seven out of the initial thirty-one features were found to be sufficient for classifying the signals.

The machine learning process is based on a DT composed of the Gini diversity index [19], the towing rule, and the maximum deviance reduction split criteria [20]. The tree starts with a root, followed by the nodes interconnected by the branches. The last nodes of the tree are called leaves, representing the final class of the disturbance. At the first node, the classifier analyses all the available features and compares them with the trained model to split the node. The number of tree branches also affects the complexity of the tree. Here, it is set to a maximum of 20 to maintain the complexity of the tree. Another concern about using the decision tree is the overfitting of data due to sharp requirements used at every node. This can be overcome by using different decision trees bagged together as ensemble trees. The method is combined with a fuzzy logic approach to make it more robust and immune to noise [5]. The *k*-fold cross-validation approach is adopted in the method, the data is partitioned into *k*-folds, and the accuracy is estimated on each fold; therefore, the overall accuracy of the method is the average of all

folds. This helps to tune the performance of the classifier to avoid overfitting. The overall accuracy, sensitivity (3) and specificity (4) evaluate the performance.

$$Sensitivity = \frac{True\ Positive}{True\ positive + False\ negative} \tag{3a}$$

$$Specificity = \frac{True\ Negative}{True\ negative + False\ positive} \tag{4}$$

To generate different scenarios, the circuit shown in Fig. 1 variates the parameters influencing ferroresonance. Increasing or decreasing the shunt capacitor >30th times, the change of parameters has different impacts on the onset of the sustained period but not in the modes. The resulting confusion matrix that shows the true positive rate of each disturbance is depicted in Fig. 9. It can be seen that the model's overall accuracy is 99.8 %. with an error of 0.2 %.

The essential metrics for the classifier's performance evaluation depend on the objective of the classification algorithm.

False tripping or no detection of disturbances can create issues in the network and the classifier. The primary aim of this paper is monitoring, with the potential for its capability to be significantly improved in the future for control activities in the network.

In that sense, after the disturbance is detected in Step 1, Step 2 is performed (see Fig. 10). The classification is performed for a specified window of three cycles. The two major steps during this stage are feature generation and new sample prediction. During this period, a sliding window is used to collect the signal data used as input for the classifier. This step is optimized by reducing the evaluation rate to 4 times per defined window. The signal length of one cycle k is acquired four times per window. This is implemented using the decision flowchart shown in Fig. 10. This approach is adopted instead of a sliding window of one data point increment to reduce the computational burden. Consequently, four predictions are obtained per window, and the final output is the common predicted class from the four predictions, reducing the false positive rate with the assumption that one disturbance occurs at a time. The class time in Fig. 10 indicates the number of windows the classification continuously uses. It is set to three cycles, and three different results are obtained, showing the first indication of the disturbance type. The expected result from the secondary and primary arcing detection is determining the arc extinction time, which is the time taken to extinguish the arc. Thus, the classification window of three cycles is too small to evaluate this. Moreover, continuous computation throughout the signal will provide redundant data and consume memory. This leads to the next step, where an adaptive time is proposed as the issue solution.

3.4. Step 3 & 4 dead times

Adaptive timing is introduced into the classification algorithm to optimize efficiency by reducing redundant data and saving computational memory.

The ferroresonance disturbance takes some time before settling into the sustained mode to be classified. At first, a dead time of 10 cycles is introduced, after which a lesser dead time (period of no computation) is proposed. During the first few cycles, all modes are classified as chaotic ferroresonance because it has a continuous transient voltage with no pattern. Step one is initiated again at the end of the pre-set time (see Fig. 11, Step 3). This is to reconfirm the presence of the disturbance after the dead period. After Step 3, the ferroresonance timing is activated (see Fig. 11, Step 4). It has five cycles as a dead time, reducing the redundant data generation. This is because the sustained period, particularly for fundamental ferroresonance, remains unchanged unless there is a modification in the system configuration, such as introducing external losses or turning off the source. Then, the ferroresonance case is stored.

Assuming k is the number of samples per window size, the detection

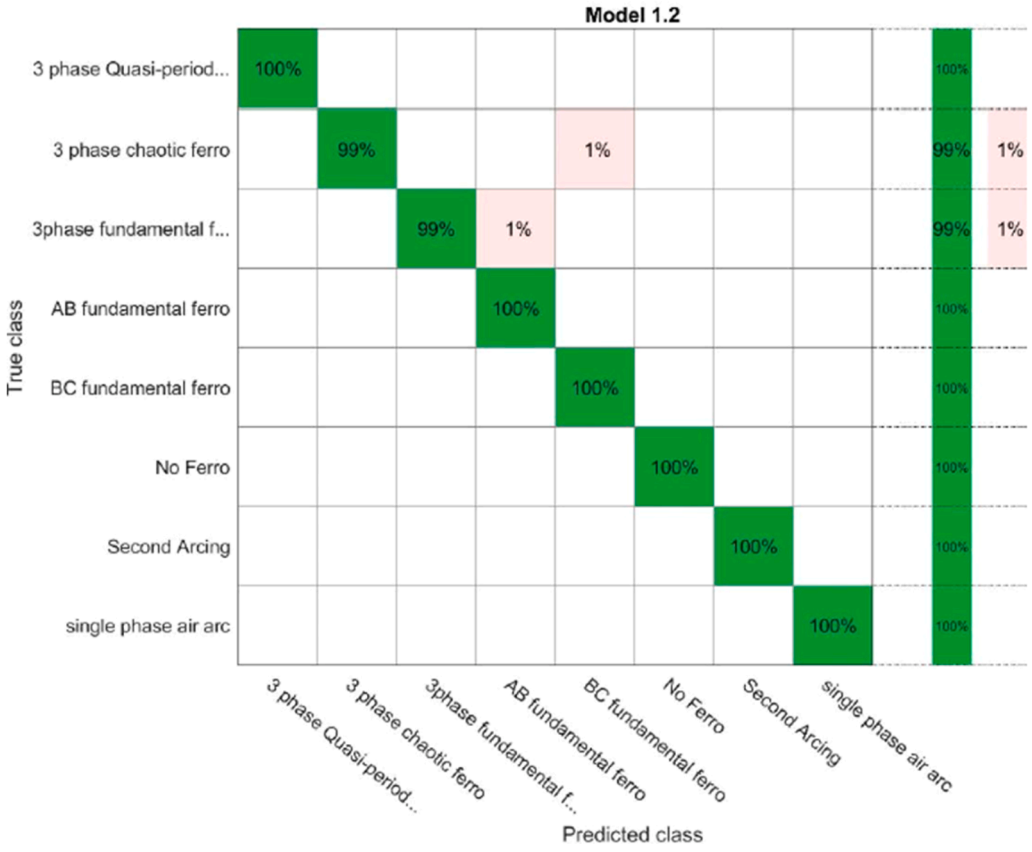

Fig. 9. Confusion matrix of trained decision tree for all disturbance classes.

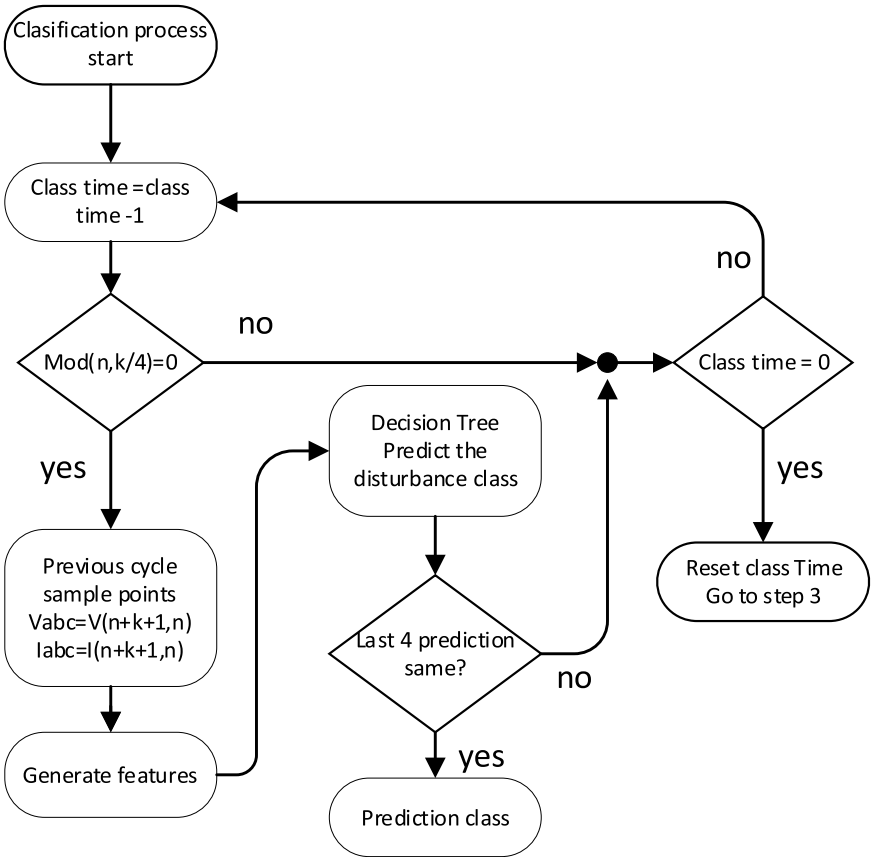

Fig. 10. Flowchart of a ferroresonance event classification procedure.

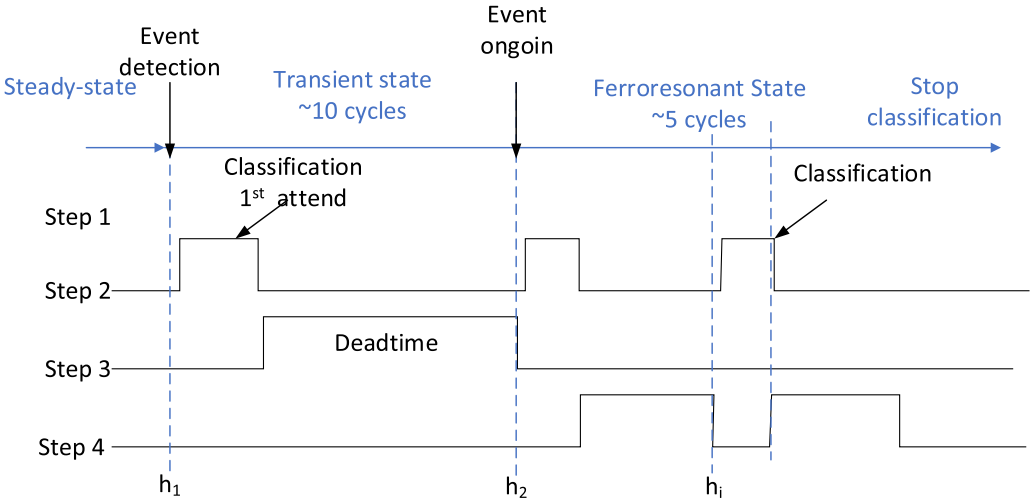

Fig. 11. On Steps during ferroresonance event.

and the classification algorithm is summarized as follows:

Detection: Compute $|\Delta I|$ and $|\Delta V|$ at the current time step. Compare these to thresholds to detect disturbances. If values exceed thresholds for up to $h + k/10$ sample points, activate classification and pause detection during this period.

Classification: Over $3k$ samples, extract features four times per window and classify disturbances, producing three outputs per window.

Dead Time: After classification, apply a 10-cycle dead time. Recheck $|\Delta I|$ and $|\Delta V|$. If disturbances persist, repeat classification ($3k$ samples), identifying the type (arcing fault or ferroresonance).

Ferroresonance: If classified as ferroresonance, apply a dead time of $5k$, followed by repeated detection and checking steps for four cycles. Terminate if no disturbance is detected.

4. Study case

To evaluate the proposed algorithm performance. The next disturbances are simulated and evaluated:

- three-phase fundamental ferroresonance,
- three-phase chaotic ferroresonance,
- AB fundamental ferroresonance,

- BC fundamental ferroresonance,
- single phase elongated air arc,
- secondary arc, and
- no ferroresonance.

The classification error is analyzed using the formula

$$P = \sum_{i}^{n} P(\omega_i) \frac{m_i}{N_i} \tag{5}$$

where m_i is the number of misclassified vectors, and N_i is the total number of vectors from class ω_i. The confusion matrix in Fig. 9, extracted from Matlab after training the classifier, presents a value of $P = 0$ for all classes except the three-phase fundamental ferroresonance and the three-phase chaotic ferroresonance. This shows that the classifier is accurate enough to classify the disturbances. Additional evaluation is done with separate signals to verify the training process's result and the adaptive timing. Fig. 12 presents the result obtained when the fundamental ferroresonance case is tested with the proposed algorithm. Each step is activated when the amplitude is 1; otherwise, it is inactive. As shown in Fig. 12, dead time ferroresonance occurs after the general dead time. After this period, the ferroresonance mode is found.

During this event, the first few cycles of the fundamental ferroresonance are classified as quasi-periodic, but after (0.5 s), the event is ascertained as Fundamental (see Table 2). The method classifies the ferroresonance in time.

5. Conclusions

This paper discusses the four common modes of ferroresonance; the fundamental, the subharmonic, the chaotic and the quasi-periodic. The frequency spectrum of the voltage and current signals is applied to categorize the signals into different modes. A step-wise implementation and adaptive dead time are proposed to reduce redundant data and save computational space. Apart from the classifier evaluation with a 25 % test dataset, the whole algorithm has been tested with >20 cases of disturbances using a combination of steady-state and post-fault data. The algorithm detects the transient inception time in less than a cycle for all cases and subsequently classifies them correctly.

Table 2
Classification results during Fundamental Ferroresonance.

Time (s)	Ferroresonance mode	Time (s)	Ferroresonance mode
0.240	Chaotic	0.620	Fundamental
0.260	Quasi-periodic	0.640	Fundamental
0.280	Quasi-periodic	0.660	Fundamental
0.500	Fundamental	0.920	Fundamental
0.520	Fundamental	0.940	Fundamental

- The algorithm's efficiency is shown by its ability to detect and classify disturbances within 100 ms.
- The successful application of adaptive dead time to ferroresonance reduces computational memory and optimizes resources by increasing the dead time interval.
- The algorithm is robust, with a high classification accuracy of 99.8 %, which is observed during system evaluation.

The method is not meant to replace primary protection functions but serves as a tool for transmission and distribution operators to detect and catalogue ferroresonance, addressing a current gap in available tools. It supports proactive monitoring by identifying early signs of specific ferroresonance modes to prevent severe damage. However, the first two steps have been developed in a way that can be implemented in real-time; the overall method has not yet been adapted for online use. Future work will focus on enabling real-time simulation.

CRediT authorship contribution statement

Aminat B. Rasheed: Investigation, Conceptualization, Writing – original draft, Formal analysis. **Jose de Jesus Chavez:** Writing – original draft, Validation, Software, Project administration, Investigation, Formal analysis, Conceptualization, Writing – review & editing, Visualization, Supervision, Resources, Methodology, Funding acquisition, Data curation. **Sarasij Das:** Writing – review & editing, Supervision, Investigation, Validation, Project administration. **Oliver Probst:** Writing – review & editing, Data curation, Supervision, Conceptualization. **Juan Carlos Cisneros Ortega:** Validation. **Marjan Popov:** Writing – original draft, Validation, Resources, Investigation, Conceptualization, Writing – review & editing, Visualization, Supervision, Methodology, Funding acquisition.

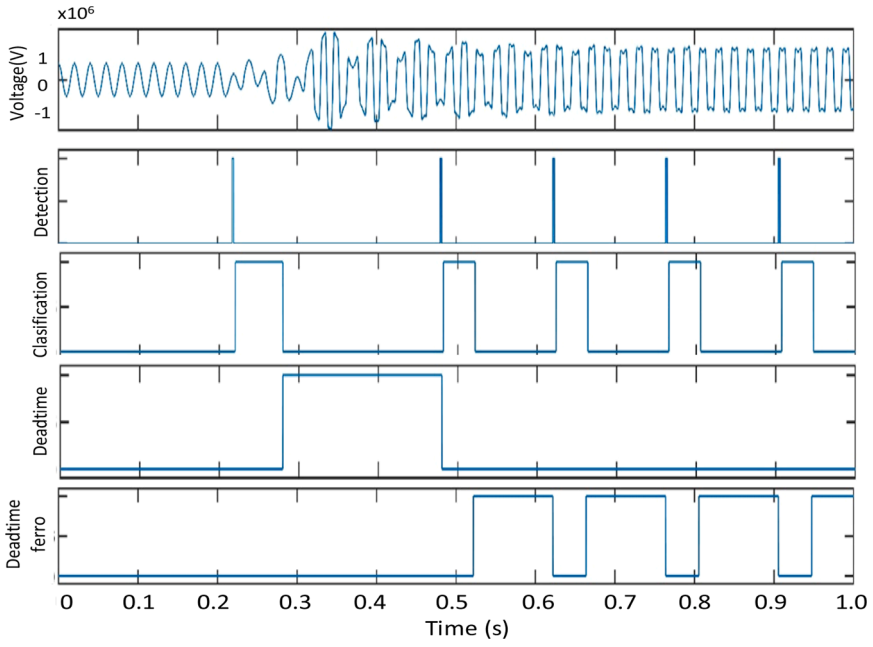

Fig. 12. Study case: Fundamental resonance event voltage signal and steps activation during the classification procedure.

Declaration of competing interest

The authors declare that they have no known competing financial interests or personal relationships that could have appeared to influence the work reported in this paper.

Apendix

Table 3
No linear load parameters: flux linkage vs current.

Current (A)	Fluxlinked (WbT)
0.0007348	180.058
0.0057800	1080.139
0.0083800	1530.284
0.0154000	1620.729
0.0273000	1710.550
0.0741600	1890.608
0.2000000	2100

Data availability

Data will be made available on request.

References

[1] R. Iravani, et al., Modeling and analysis guidelines for slow transients. III. The study of ferroresonance, IEEE Trans. Power Delivery 15 (1) (Jan. 2000) 255–265, https://doi.org/10.1109/61.847260.

[2] P. Boucherot, Existence de deux regimes en ferroresonance, Rev. Gen. de L'Elec 8 (24) (1920) 827–828.

[3] D.A.N. Jacobson, Examples of ferroresonance in a high voltage power system, in: 2003 *IEEE Power Engineering Society General Meeting*, IEEE, 2003. Cat. No. 03CH37491.

[4] G. Mokryani, M.-R. Haghifam, J. Esmaeilpoor, Identification of ferroresonance based on wavelet transform and artificial neural network, Eur. Trans. Electr. Power 19 (3) (2009) 474–486.

[5] G. Mokryani, P. Siano, A. Piccolo, Identification of ferroresonance based on S-transform and support vector machine, Simul. Model. Pract. Theory. 18 (9) (2010) 1412–1424.

[6] S. Beheshtaein, Application of wavelet-base method and DT in detection of ferroresonance from other transient phenomena, in: 2012 *International Symposium on Innovations in Intelligent Systems and Applications*, 2012.

[7] H.A. Sharbain, A. Osman, A. El-Hag, Detection and identification of ferroresonance, in: 2017 7th International Conference on Modeling, Simulation, and Applied Optimization (ICMSAO), Sharjah, United Arab Emirates, 2017, pp. 1–4, https://doi.org/10.1109/ICMSAO.2017.7934904.

[8] Z. Kang, Longchen Li, Classification and recognition of ferroresonance based on improved Elman-Adaboost, Res. Sq. (2023), https://doi.org/10.21203/rs.3.rs-2864538/v1.

[9] H.S. Nogay, T.C. Akinci, M.I. Akbas, A. Tokić, Diagnosis of chaotic ferroresonance phenomena using deep learning, IEEe Access. 11 (2023) 58937–58946, https://doi.org/10.1109/ACCESS.2023.3285816.

[10] D.M. Kim Breitfelder, IEEE 100: The Authoritative Dictionary of IEEE Standards Terms, the United States of America, IEEE Press publications, 2000.

[11] M. Zou, Accurate simulation model for a three-phase ferroresonant circuit in EMTP–ATP, Int. J. Electr. Power Energy Syst. 107 (2019) 68–77.

[12] M. Tajdinian, M. Allahbakhshi, S. Biswal, O.P. Malik, D. Behi, Study of the impact of switching transient overvoltages on ferroresonance of CCVT in series and shunt compensated power systems, IEEE Trans. Ind. Informatics 16 (8) (2020) 5032–5041.

[13] S.P. Ang, Z.D. Wang, P. Jarman, M. Osborne, Power transformer ferroresonance suppression by shunt reactor switching, in: 2009 44th International Universities Power Engineering Conference (UPEC), 2009.

[14] Tongxin Zheng, E.B. Makram, A.A. Girgis, Power system transient and harmonic studies using wavelet transform, in: IEEE Transactions on Power Delivery, 14, Oct. 1999, pp. 1461–1468, https://doi.org/10.1109/61.796241.

[15] K.S. Thyagarajan, Discrete wavelet transform," in still image and video compression with MATLAB, IEEE (2011) 99–131, https://doi.org/10.1002/9780470886922.ch4.

[16] P.H.A.S. Swain, Using superimposed principles (Delta) in protection techniques in an increasingly challenging power network, in: 2017 70th *Annual Conference for Protective Relay Engineers* (CPRE), Texas, 2017.

[17] J. Zhang, H. Jia, N. Zhang, Alternate support vector machine decision trees for power systems rule extractions, IEEE *Trans. Power Syst.* 38 (1) (Jan. 2023) 980–983, https://doi.org/10.1109/TPWRS.2022.3220088.

[18] J. Upendar, C.P. Gupta, G.K. Singh, Statistical decision-tree based fault classification scheme for protection of power transmission lines, Int. J. Electr. Power & Energy Systems 36 (1) (2012) 1–12, https://doi.org/10.1016/j.ijepes.2011.08.005. ISSN 0142-0615.

[19] M. Hassan, et al., GITM: a GINI index-based trust mechanism to mitigate and isolate sybil attack in RPL-enabled smart grid advanced metering infrastructures, IEEe Access. 11 (2023) 62697–62720, https://doi.org/10.1109/ACCESS.2023.3286536.

[20] M.M. Badr, M.S. Hamad, A.S. Abdel-Khalik, R.A. Hamdy, S. Ahmed, E. Hamdan, Fault identification of photovoltaic array based on machine learning classifiers, IEEe Access. 9 (2021) 159113–159132, https://doi.org/10.1109/ACCESS.2021.3130889.